Improving the Availability of Tandem Hot Metal Strip Rolling

THE USE OF FAULT-TOLERANT TECHNIQUES WITH VIRTUAL ROLLING

By John Pittner and Marwan A. Simaan

IT IS IMPORTANT IN THE CONTROL OF THE TANDEM rolling of hot metal strip to achieve a degree of robustness to faults in certain measurements to avoid degradation of the availability of the process. Examples of such faults are those that would preclude valid measurements in strip tension and roll force. These types of faults could degrade the process availability and seriously reduce the quality and yield of the output, along with a major loss of production and possible equipment damage. In this article, we propose a method of control for this process that permits continuity of operation during possible faults in the tension or roll force measurements and without major disruptions in process operation or significant reduction in the quality of the output. The effectiveness of this method is shown by simulations using data from an operating mill.

Overview

In earlier work [1], [2], we have developed advanced controllers for the tandem hot and cold metal strip rolling processes. The tandem rolling of hot metal strip (Figure 1) is a major manufacturing process in which hot metal bars are reduced in thickness by being compressed in a series of mill stands. Each stand consists of a pair of independently driven work rolls supported by backup rolls of larger diameter. A device denoted as a looper (Figure 2) is located between two adjacent stands. The looper supports the control of tension in the hot strip by using hydraulics and an arm and pivot arrangement to apply force against the moving strip.

A measurement of roll force is provided at each mill stand, and of strip tension between each set of adjacent stands. Generally, these measurements are made by sensors that produce signals to instrumentation channels that feed the measured variables to the controller. The deviation

Digital Object Identifier 10.1109/MIAS.2018.2875216
Date of publication: 26 April 2019

1077-2618/19©2019IEEE

of a measured variable from a desired value by a predetermined amount can be caused by an abnormal operation of a sensor or a fault in the associated instrument channel. To be effective, the controller must be robust to faults that are fast acting or develop slowly. A significant degradation in the quality of the mill output or, more seriously, a major loss in production and possible equipment damage due to a fault can result from the failure of the controller to mitigate such faults.

The results of our work are described herein, where a controller is enhanced by a virtual rolling function to provide robustness to these faults and thus allow continued operation of the mill in the presence of one or both of these faults. Table 1 lists the symbols used unless otherwise noted.

Mathematical Process Model

A mathematical model [4], [5] of the threaded mill has been developed and verified. As described in [4]–[6], the significant features of this model are presented in what follows. It is assumed for this investigation that a method of active compensation for mill roll eccentricity is operable so that any eccentricity components remaining after compensation are insignificant and that Young's modulus, workpiece width, and density are constant.

During normal running, the operating point of the mill is based on a fully threaded condition at operating speed with a strip tension of 0.01 kN/mm^2 between adjacent stands and with each looper at an angle of 15°. Table 2, which is actual data from an operating plant [7], lists the operating point strip thickness h_{out}, the average strip temperature T at the mill entry and at the exit of each stand, the peripheral speed V_0 of the work rolls, and the undeformed work roll radius R of each stand.

The roll force in the roll bite (i.e., the area between the work rolls where the strip thickness is reduced) is estimated using Sims's model [8]. The model is enhanced by using the empirical results of Shida [9] to better estimate the resistance to deformation of the material being rolled. In Sims's model, the specific roll force is represented as

$$P = (kQ_p - \bar{\sigma})\sqrt{R_p \delta}, \tag{1}$$

where Q_p is a factor that compensates for friction and any inhomogeneities of deformation, and R_p is estimated using the Hitchcock approximation [10]. The exit thickness h_{out} is estimated using the linearized relation for the output thickness as

$$h_{\mathrm{out}} = S + S_0 + \frac{F}{M}, \tag{2}$$

where the total rolling force $F = PW$, and M represents the elastic stretch of the mill stand under the application of F.

The forward slip f is a measure of the strip speed exiting the roll bite and is defined as

$$f = \frac{V_{\mathrm{out}} - V_0}{V_0}. \tag{3}$$

A model presented in Ford et al. [11] for the forward slip in cold metal rolling is more useful for control development, except that for hot rolling, the empirical relationship given in Roberts [12] for the coefficient of sticking friction is used in place of the coefficient for sliding friction, which is used for cold rolling.

A model for strip tension is derived from the relationship for Young's modulus

$$\frac{d\sigma}{dt} = \frac{E}{L_0}\left[\frac{dL(\theta(t))}{dt} + V_{\mathrm{in},i+1} - V_{\mathrm{out},i}\right], \ \sigma(0) = \sigma_0. \tag{4}$$

The position of the hydraulic cylinder that sets the work roll position at the roll bite and the peripheral speed of the work rolls are modeled as single first-order lags

$$\frac{dS}{dt} = \frac{U_S}{\tau_S} - \frac{S}{\tau_S}, \quad S(0) = S_0, \tag{5}$$

$$\frac{dV}{dt} = \frac{U_V}{\tau_V} - \frac{V}{\tau_V}, \quad V(0) = V_0. \tag{6}$$

The interstand time delay is the time taken for an element of strip to move between adjacent stands and is approximated as

$$\tau_{d,i,i+1} = \frac{L}{V_{\mathrm{out},i}}. \tag{7}$$

The looper position angle is determined as

$$\frac{d\theta}{dt} = \omega, \ \theta(0) = \theta_0, \tag{8}$$

where ω is derived from Newton's second law of motion as

$$\frac{d\omega}{dt} = \frac{1}{J_{\mathrm{lpr}}}[M_{\mathrm{lpr}} + M_{\mathrm{fct}} + M_{\mathrm{ld}}], \quad \omega(0) = 0, \tag{9}$$

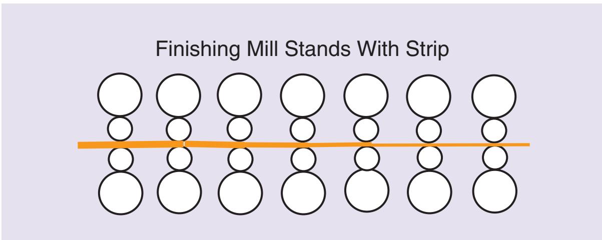

FIGURE 1. A typical tandem hot strip finishing mill [2].

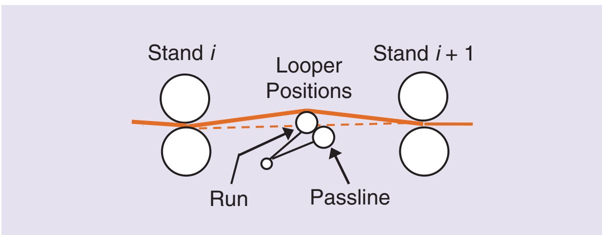

FIGURE 2. The looper schematic [3].

Table 1. Nomenclature

$A(x)$: State-dependent matrix
B: Control matrix
BA: Subscript, basic regime
$C(x)$: State-dependent output matrix
E: Young's modulus
e: Subscript, estimated value
F: Total rolling force
f: Forward slip
h: Strip thickness
i: Subscript, stand i
in: Subscript, stand input
J: Performance index
J_{lpr}: Looper moment of inertia
$K(x)$: Solution to Riccati equation
k: Constrained yield stress
k_{vis}: Viscous friction constant
L_0: Length between center line of stands
L: Strip length between stands
L: Superscript, left inverse
M: Mill modulus
M_{bnd}: Looper torque, bending
M_{fct}: Looper torque, friction
M_{ld}: Looper torque, total load
M_{lmas}: Looper torque, looper mass
M_{lpr}: Torque applied to looper
M_{swt}: Looper torque, strip weight
M_{ten}: Looper torque, strip tension
o or op: Subscript, operating point value
out: Subscript, stand output value
P: Specific roll force
PR: Subscript, preroll regime
$Q(x)$: State-weighting matrix
R: Undeformed work roll radius
R: Subscript, roll regime
R_p: Deformed work roll radius
$R(x)$: Control-weighting matrix
S: Roll gap actuator position
S_0: Intercept of mill stretch approximation
T: Strip temperature (°C)
t: Time (s)
U_{Mlpr}: Looper torque controller reference
U_S: Roll gap actuator reference
U_V: Work roll speed actuator reference
u: Control vector
V_0: Work roll peripheral speed
V: Strip speed
W: Strip width
x: State vector
y: Output vector
δ: Draft $= h_{\text{in}} - h_{\text{out}}$
θ: Looper angle
σ: Tension stress
$\bar{\sigma}$: Average tension stress $= (\sigma_{\text{in}} + \sigma_{\text{out}})/2$
τ_d: Interstand time delay
τ_M: Time constant, looper torque controller
τ_S: Time constant, roll gap position controller
τ_V: Time constant, work roll speed controller
ω: Looper angular velocity
A': Indicates transpose of matrix A
$\in C^k$: Elements of matrix or vector has continuous partial derivatives through order k

Table 2. The mill operating point

Stand	h_{out} (mm)	T (°C)	V_0 (m/s)	R (mm)
Entry	38.8	1,058	—	—
1	21.6	988	1.188	360
2	14.4	973	1.823	336
3	8.6	957	2.957	353
4	6.1	938	4.294	343
5	4.7	922	5.665	388
6	3.9	904	6.946	348
7	3.5	894	7.880	369

with $M_{\text{ld}} = M_{\text{ten}} + M_{\text{swt}} + M_{\text{lmas}} + M_{\text{bnd}}$. The steady-state values of the torques and the value of J_{lpr} are as given in "Looper Characteristics." The torque M_{lpr} is approximated as a first-order lag that includes the looper hydraulic cylinder with its controller

$$\frac{dM_{\text{lpr}}}{dt} = \frac{U_{M_{\text{lpr}}}}{\tau_M} - \frac{M_{\text{lpr}}}{\tau_M}, \quad M_{\text{lpr}}(0) = M_{\text{lpr},0}. \tag{10}$$

The friction torque of the looper mechanism is approximated for this investigation as

$$M_{\text{fct}} = k_{\text{vis}}\omega. \tag{11}$$

Detailed calculations for the looper torques, moment of inertia, and $dL(\Theta(t))/dt$ are as given in [2].

For use in the simulation of the controller, the previous relationships are expressed in state-space form as

$$\frac{dx}{dt} = A(x)x + Bu, \quad x(0) = x_0, \tag{12}$$

$$y = C(x)x, \tag{13}$$

where $x \in R^n$ is a vector whose elements represent the individual state variables, $u \in R^m$ is a vector whose elements represent the individual control variables, $y \in R^p$ is a vector whose elements represent the individual output variables, $A(x) \in R^{\text{nxn}}$ and $C(x) \in R^{\text{pxn}}$ are state-dependent matrices, and $\text{B} \in R^{\text{nxm}}$ is a constant matrix. The elements of the $A(x)$, $C(x)$, and B matrices are as determined in our previous work [2]. The variables represented by the elements of the state, control, and output vectors, where U represents a control reference, are represented as shown in Table 3 [6]. All of the states are available at the controller because the variables represented by the elements of the state vector are derived from direct measurements.

The Controller

Brief Description of the Control Strategy

The following assumptions, typical of actual operational situations, are used in the evaluation of the controller: a fault occurs in the measurement of tension between stands 1 and 2, a fault occurs in the measurement of the roll force at stand 1, that these faults might occur separately or together, and with the rest of the process functioning normally. The continued operation of the mill requires that these measurements remain unfaulty. They were selected for this initial evaluation because their simulation in the model is fairly straightforward, and they could provide a reasonable basis for the future evaluation of similar scenarios involving faults because the methodology developed herein would be applicable. This would include the means to easily estimate the conditions under which nearly normal operation of the mill could be retained in the presence of faulted measurements. A functional schematic of the overall control technique is presented in Figure 3, wherein, during normal operation, the tension and roll force measurements are used to determine the tension stress and the specific roll force. The variables denoted as virtual tension and virtual roll force are generated by (4) and (1) in the mill model. The switching logic, the thickness estimate (2), and the model are physically located together in the controller but are shown separately for clarity. Because the model is based on a wide range of data from actual installations and considerable experience, it represents the actual process reasonably well. Thus, any deviations between the model and the actual process are minor but not negligible, and similarly for deviations between the virtual and the actual measurements. The interfacing signals are from local functions, local controllers, actuators, and sensors, e.g., looper torques

Looper Characteristics

The dimensions as shown in Figure S1 [4]: L_0 = 5.478 m, y = 0.191 m, a = 1.943 m, r(radius) = 0.152 m, l = 0.762 m. Max angle: 40°. Pass line angle: 2.9°. Mass of looper arm: 300 kg. Mass of looper roll: 500 kg. Viscous friction constant: k_{vis} = –2.0 kNm/rad/s. Moment of inertia: J_{lpr} = 0.3542 (in kgm²/1,000). At the steady-state operating point: θ = 15°, ω = 0 rad/s, $l1$ = 2.684 m, $l2$ = 2.806 m, M_{ten} = –4.289 kNm, M_{swt} = –1.515 kNm, M_{lmas} = –4.693 kNm, M_{bnd} = –0.132 kNm, M_{fct} = 0 kNm, M_{ld} = –10.629 kNm, and M_{lpr} = 10.629 kNm.

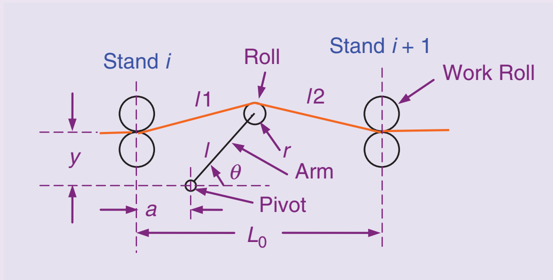

FIGURE S1. The looper detail [4].

Table 3. The state, control, and output vector variable assignments

State Vector		Control Vector	Output Vector	
x_1 (σ_{12})	x_{21} (M_{12})	u_1 (U_{S1})	y_1 (h_{out1})	y_{14} (P_1)
x_2 (σ_{23})	x_{22} (M_{23})	u_2 (U_{S2})	y_2 (h_{out2})	y_{15} (P_2)
x_3 (σ_{34})	x_{23} (M_{34})	u_3 (U_{S3})	y_3 (h_{out3})	y_{16} (P_3)
x_4 (σ_{45})	x_{24} (M_{45})	u_4 (U_{S4})	y_4 (h_{out4})	y_{17} (P_4)
x_5 (σ_{56})	x_{25} (M_{56})	u_5 (U_{S5})	y_5 (h_{out5})	y_{18} (P_5)
x_6 (σ_{67})	x_{26} (M_{67})	u_6 (U_{S6})	y_6 (h_{out6})	y_{19} (P_6)
x_7 (S_1)	x_{27} (θ_{12})	u_7 (U_{S7})	y_7 (h_{out7})	y_{20} (P_7)
x_8 (S_2)	x_{28} (θ_{23})	u_8 (U_{V1})	y_8 (σ_{12})	y_{21} (θ_{12})
x_9 (S_3)	x_{29} (θ_{34})	u_9 (U_{V2})	y_9 (σ_{23})	y_{22} (θ_{23})
x_{10} (S_4)	x_{30} (θ_{45})	u_{10} (U_{V3})	y_{10} (σ_{34})	y_{23} (θ_{34})
x_{11} (S_5)	x_{31} (θ_{56})	u_{11} (U_{V4})	y_{11} (σ_{45})	y_{24} (θ_{45})
x_{12} (S_6)	x_{32} (θ_{67})	u_{12} (U_{V5})	y_{12} (σ_{56})	y_{25} (θ_{56})
x_{13} (S_7)	x_{33} (ω_{12})	u_{13} (U_{V6})	y_{13} (σ_{67})	y_{26} (θ_{67})
x_{14} (V_1)	x_{34} (ω_{23})	u_{14} (U_{V7})		
x_{15} (V_2)	x_{35} (ω_{34})	u_{15} (U_{Mlpr12})		
x_{16} (V_3)	x_{36} (ω_{45})	u_{16} (U_{Mlpr23})		
x_{17} (V_4)	x_{37} (ω_{56})	u_{17} (U_{Mlpr34})		
x_{18} (V_5)	x_{38} (ω_{67})	u_{18} (U_{Mlpr45})		
x_{19} (V_6)		u_{19} (U_{Mlpr56})		
x_{20} (V_7)		u_{20} (U_{Mlpr67})		

and positions, roll bite cylinder positions, and work roll speeds. These are devices that, during actual operation, have a close interaction with the strip.

The switching logic switches the tension feedback from measured tension to virtual tension when the virtual tension is outside an acceptable operating range. Virtual tension is computed in the model (4) based on interfacing signals from the process and is used because the tension measurement is less reliable as it is more susceptible to faults. The closed-loop control after switching is based on virtual tension. Thus, there is an uninterrupted processing of the strip in the mill with little likelihood of a wreck with possible equipment damage and loss of production or a serious degradation of the quality of the output due to highly undesirable excursions in tension. However, some degradation could still be expected because the uncertainty in the virtual tension is greater than in the measured tension. In this case, the quality of the final product is generally useful, although possibly in a limited sense, and it might be somewhat degraded from that processed with a healthy measurement, depending on the product.

The estimated gain of the roll force measurement is the basis for switching the roll force from measured to virtual. This is because the desired roll force is not set by a fixed reference but instead can change depending on various operational situations, such as changes in the resistance to deformation of the strip. Thus, the roll force gain, as determined by the measured roll force/virtual roll force, is used so that, if the roll force gain is outside a specified range, a switch is made from the measured roll force to the virtual roll force. The simulations provide additional characteristics of the control of tension and roll force.

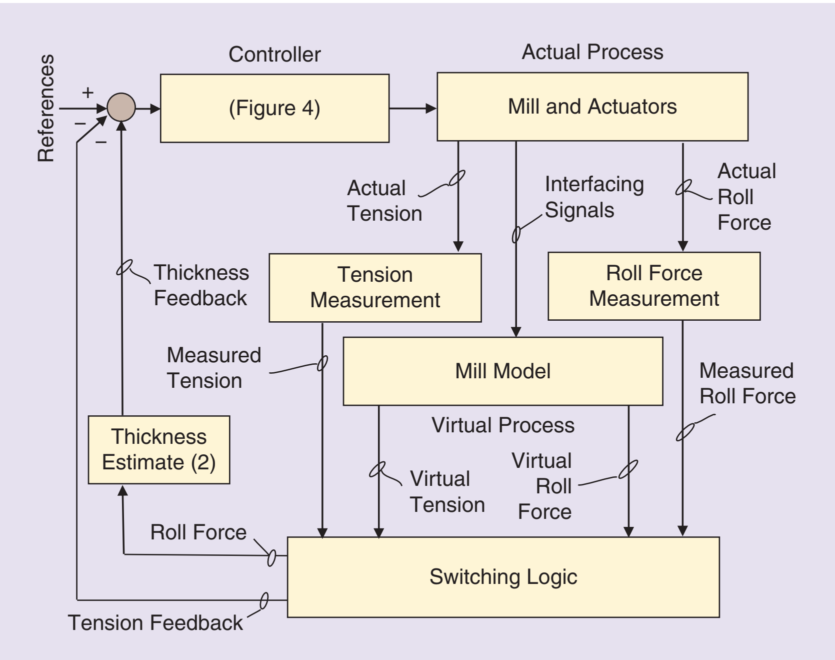

FIGURE 3. The controller functional schematic [6].

Uncertainties and Disturbances

The initial development of the control strategy is based on zero uncertainties and disturbances to verify the overall control concept. However, during realistic scenarios, uncertainties and disturbances must be considered to assure the proper functioning of the controller. Based on experience, what is available commercially in force measurement, and conservative calculations based on [13], the uncertainty in the tension measurement is taken to be about ±5% of the actual tension and about ±10% for the virtual estimate. Similarly, an uncertainty in the roll force measurement is taken to be about ±5% of the actual roll force and about ±10% for the virtual estimate.

An acceptable operating range of the tension to reduce the likelihood of false faults, considering uncertainties in the virtual and the measurement, is taken as 0.0121 and 0.0081 kN/mm^2 in the virtual tension. This is based on a reference in the actual tension of 0.01 kN/mm^2. In certain cases, this range could result in a slight increase in tension excursions with only a minor impact on the product. An acceptable operating range of the gain in the roll force measurement, which is based on a reference gain of 1 and considers the uncertainties in the measurement and in the virtual estimate, is taken as 0.65–1.35. The tension could be affected by disturbances in the looper torque, and the roll force could be affected by disturbances in the entry strip thickness. These disturbances as shown in the simulation are handled well by the controller irrespective of whether the measurement is virtual or actual.

Advantages of This Technique

This technique is novel for this process, robust to false measurements, and easily implemented. This is mostly due to the use of a virtual function that was developed previously for the threading of the mill [3], so that a single virtual function can serve a dual purpose without requiring additional major functions. Furthermore, this method is friendly to commissioning and maintenance personnel who have limited backgrounds in advanced control theory, and it can handle a broad range of faults with little complexity. In the event of a fault, this reconfigured system enables the process to continue without wrecks or equipment damage, with only a possible limited effect on product quality.

Controller Structure

The state-dependent Riccati equation (SDRE) technique [14]–[18] is the basis of the controller design. The main features of this method as presented in [2] and as modified for this process are summarized in the following.

The nonlinear plant dynamics are expressed in the form as noted in (12) and (13). The optimal control problem then is defined in terms of minimizing the performance index

$$J = \frac{1}{2}\int_0^\infty (x'Q(x)x + u'R(x)u)\,dt, \tag{14}$$

with respect to the control vector u, subject to the constraint (12). The state-dependent algebraic Riccati equation (ARE)

$$A'(x)K(x) + K(x)A(x) - K(x)B\,R^{-1}(x)B'K(x) + Q(x) = 0, \tag{15}$$

is solved pointwise for $K(x)$, and $A(x)$ and B are as previously noted in (12). This results in the control law

$$u = -S(x)x, \tag{16}$$

where, for the general case,

$$S(x) = R^{-1}(x)B'K(x). \tag{17}$$

In this process, the B matrix is constant, and the Q and R matrices are diagonal with constant elements. The elements of the Q matrix are chosen to emphasize (i.e., penalize) the states representing tensions because these are somewhat more important in the process. R is an identity matrix (positive definite) to assure the existence of its inverse. The overall structure of the controller, as modified for this application to include the features of Figure 3, is depicted in Figure 4.

Each element of the state vector x is measurable, y_e is a vector whose elements are the measured (or estimated) elements of y, and φ_y is an algorithm that generates y_e. The K_P and K_I blocks represent diagonal matrices whose elements are the proportional and integral gains for the thickness and tension trims. The settings of the elements are determined intuitively using the designer's preferred procedure, after the establishment of the SDRE control law, to provide a steady-state zero-error response and a user-friendly means of final adjustment as needed at installation. The looper operating point trims are implemented by the algorithm ϕ_r. This provides a trim for the reference for the control of each looper and a direct feedthrough for other references. The process model is used for the simulation of the virtual mill and in the control of the actual mill. The logic for switching of signals from real to virtual is done by the block noted for this function. This also provides a direct feedthrough for signals not being switched.

The controller has three regimes of operation: 1) basic, 2) preroll, and 3) roll. In the basic regime, an offline simulation of a typical process operating at a typical operating point x_0 is established. Using the process model and the values of the elements of x_0, the elements of $A(x_0)$ and $C(x_0)$ are computed. The results are used to obtain a suitable controller that includes determination of the elements of the diagonal Q and R weighting matrices and the settings of the PI gains of the trims. The ARE is solved offline to determine a gain $S_{BA}(x_0)$ for the control law of the inner control loop of the controller, where

$$S_{BA}(x_0) = R^{-1}B'K(x_0) \tag{18}$$

and $K(x_0)$ is the solution of the ARE at x_0.

In the preroll regime, just prior to when the transfer bar enters the mill for threading, the model is updated by a separate system based on data collected during recent

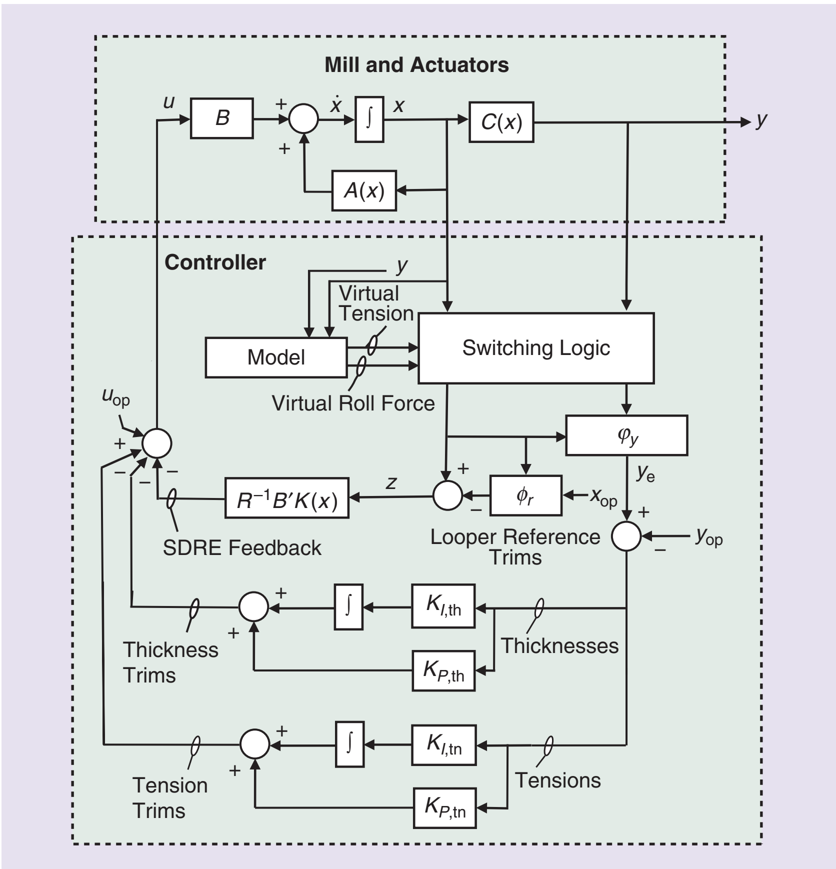

FIGURE 4. The controller structure as modified [6].

processing. Mathematical matching of the ordinary differential equations that describe the closed-loop dynamics in the basic regime with those in the preroll regime determines the controller gain as

$$S_{\mathrm{PR}}(x_0) = B^{-L}(A_{\mathrm{PR}}(x_0) - A_{\mathrm{BA}}(x_0)) + S_{\mathrm{BA}}(x_0), \qquad (19)$$

where $A_{\mathrm{PR}}(x_0)$ is determined from the updated model at the operating point of the preroll regime, $A_{\mathrm{BA}}(x_0)$ and $S_{\mathrm{BA}}(x_0)$ are as previously determined for the basic regime, B^{-L} is a left inverse of the B matrix, which inverse exits and is computed as $B^{-L} = (B'B)^{-1}B'$, and where the $A_{\mathrm{PR}}(x_0)$, $A_{\mathrm{BA}}(x_0)$, and B correspond to the A and B matrices in (12) for the preroll and basic regimes.

In the roll regime, as the strip is processed through the mill, the settings of the pointwise controller are adjusted at small successive instances of time, or points. The setting at a point j is determined by the measurement of the variables represented by the elements of the state vector at the particular instant j. At the first point ($j = 1$), the values of the $A_{\mathrm{PR}}(x_0)$ and $S_{\mathrm{PR}}(x_0)$ matrices are used to determine the inner control loop feedback gain as

$$S_{R,1}(x) = B^{-L}(A_{R,1}(x) - A_{\mathrm{PR}}(x_0)) + S_{\mathrm{PR}}(x_0). \qquad (20)$$

For subsequent points ($j = 2, 3, 4, \ldots$), the value of the inner control loop feedback gain is determined as

$$S_{R,j}(x) = B^{-L}(A_{R,j}(x) - A_{R,j-1}(x)) + S_{R,j-1}(x). \qquad (21)$$

During the processing of the remainder of the strip, this is repeated in a pointwise manner so that the controller dynamics remain essentially unchanged. Similarly, by appropriately setting the gains of the *PI* trims in consideration of the pertinent elements of the $C(x)$ matrix, the dynamic characteristics of the outer control loop are kept very nearly invariant.

Simulations

The simulations were done using MATLAB/Simulink. Initial simulations to verify the main concepts of the control technique without uncertainties or disturbances that addressed faults in the tension measurement and the roll force measurement were performed. Figure 5(a)–(d) and Figure 6 depict the results. In these figures, the excursion in the strip thickness for the fault in the tension measurement is negligible with respect to the excursion in the thickness for the fault in the roll force measurement and therefore does not show in the figures for strip thickness. Figure 5(a)–(d) and Figure 6 depict responses to a fault in the stand 1 roll force measurement and in the measurement of tension between stands 1 and 2. In Figure 6, the roll force measurement gain is similar to the roll force gain in Figure 5(c) except with an increase in the positive direction. As these figures show, good performance is retained for both actual and virtual tensions and roll forces because these faults are handled successfully by the controller. Further, excursions in the tension during a fault in the roll force measurement are minor, and similarly in the roll force for a fault in the tension measurement. The magnitudes of the peaks of excursions in the estimated strip thickness are not excessive.

Simulations were performed to evaluate performance in the presence of uncertainties and disturbances, which

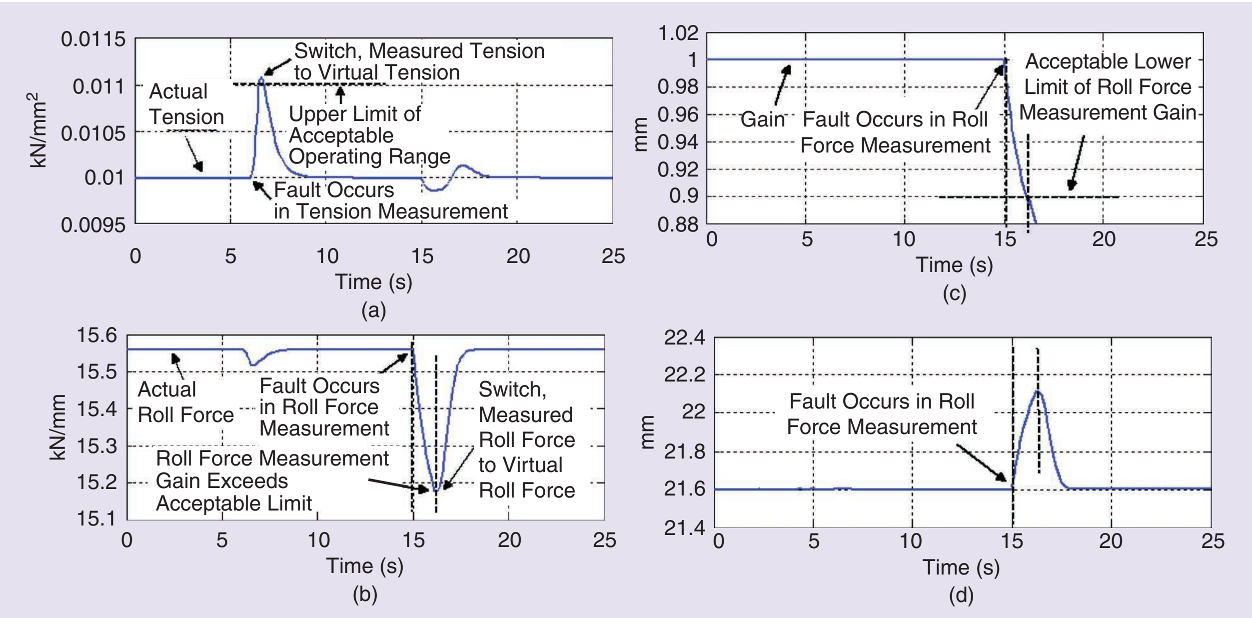

FIGURE 5. The responses for a fault in tension measurement, followed by a fault in specific roll force measurement, without uncertainties or disturbances [6]. (a) Actual tension stress, stands 1 and 2; (b) actual specific roll force, stand 1; (c) roll force measurement gain, stand 1; and (d) strip exit thickness, stand 1.

are similar to those performed previously without uncertainties or disturbances. Typical results are depicted in the following example. For the roll force, an uncertainty of −5% was applied at 5 s, with a fault in the measurement applied at 15 s and a −10% uncertainty in the virtual roll force applied at 5 s. A tension with an uncertainty of −5% was applied during the entire simulation with no fault applied in the measurement. The results are depicted in Figures 7–9. When the gain of the roll force measurement exceeds an acceptable limit, a switch is made (Figure 7) to the virtual roll force. The roll force gain using virtual roll force is shown in Figure 8. The closed-loop action of the controller (Figure 3) reduces excursions in the actual roll force and the strip thickness at the exit of stand 1 (Figure 9).

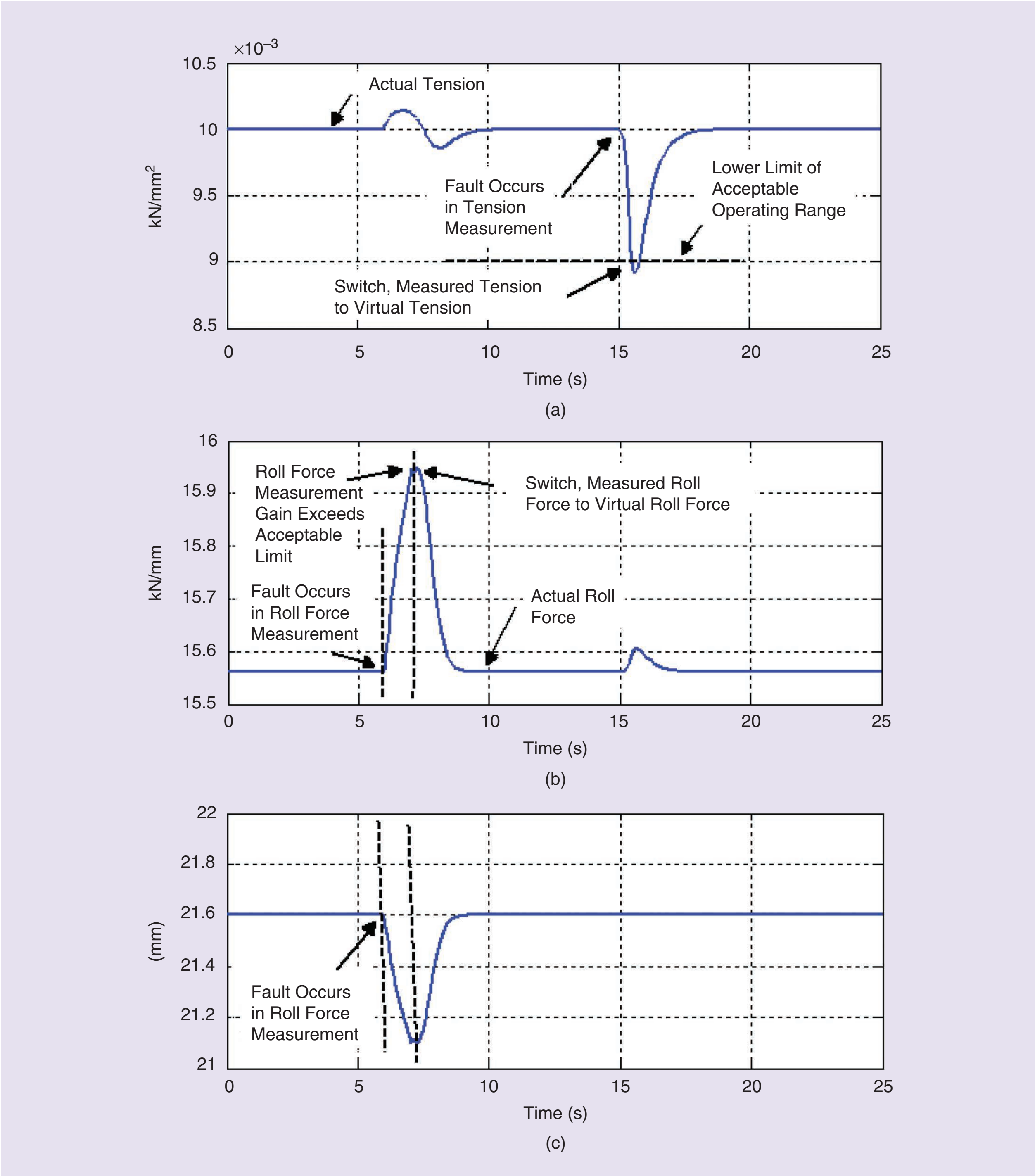

FIGURE 6. The responses for a fault in specific roll force measurement, followed by a fault in tension measurement, without uncertainties or disturbances [6]. (a) Actual tension stress, stands 1 and 2; (b) actual specific roll force, stand 1; and (c) strip exit thickness, stand 1.

The peak excursion in the actual roll force is about 5.5% above the initial value. The final value is about 2% below the initial value. The peak excursion in the strip thickness is about 5% below the initial value. The final value is about 2.3% above the initial value. During a fault in the roll force measurement, the only excursions in the tension are minor and essentially the same as depicted in Figure 6. Similar results are obtained for simulations with various other uncertainties in the roll force. The addition of unmodeled disturbances in the entry thickness is depicted in Figure 10; as shown in this figure, these disturbances are well handled for both measured and virtual roll forces.

Good performance is retained for both actual and virtual tensions and roll forces.

Simulations were done for uncertainties in the tension that were similar to those performed for the roll force. As an example, a typical case is depicted in Figure 11(a) and (b). Initially, an uncertainty of −5% in the measured tension and an uncertainty of +10% in the virtual tension were applied. Also, an uncertainty of +5% in the roll force was applied at 5 s and retained during the entire simulation. No fault was applied in the force measurement. A fault in measured tension was initiated at 15 s. This caused a decrease in the gain of the tension measurement with a corresponding increase in the actual tension because of closed-loop control action (Figure 3) to hold the tension feedback at the reference value. The virtual tension followed the actual tension with a 10% uncertainty.

When a fault is detected due to the actual tension exceeding the upper limit of its operating range, a switch is made

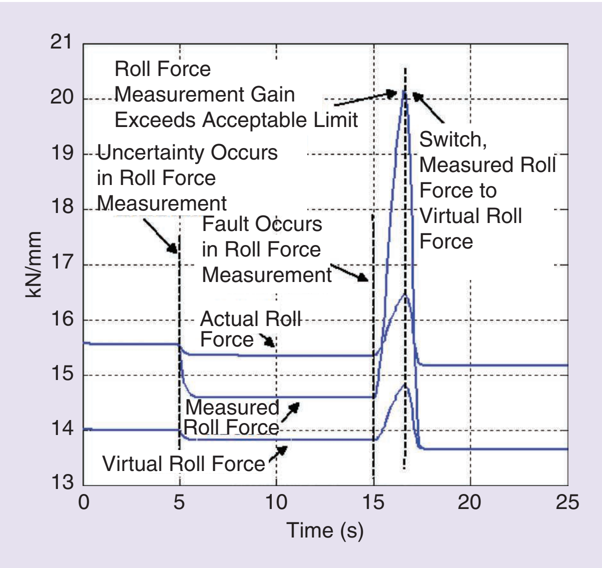

FIGURE 7. The responses for a fault in specific roll force measurement, with uncertainties [6]: the actual, virtual, and specific roll force with an uncertainty and a fault in roll force measurement, stand 1.

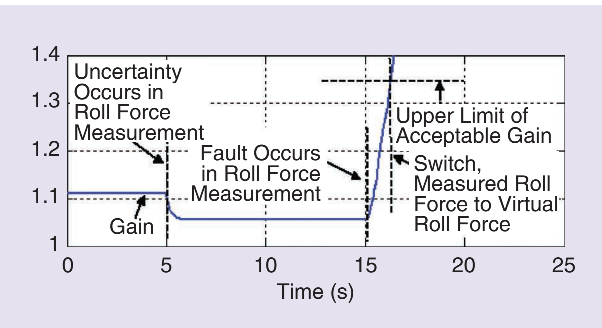

FIGURE 8. The roll force measurement gain, with uncertainties [6]: gain, based on virtual roll force, for uncertainty in roll force measurement and a fault in roll force measurement, stand 1.

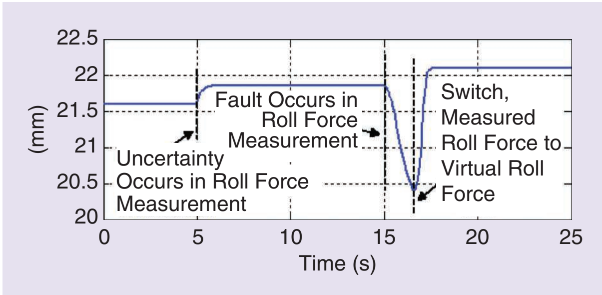

FIGURE 9. The strip exit thickness, stand 1, response to a fault in the roll force measurement, with uncertainties [6].

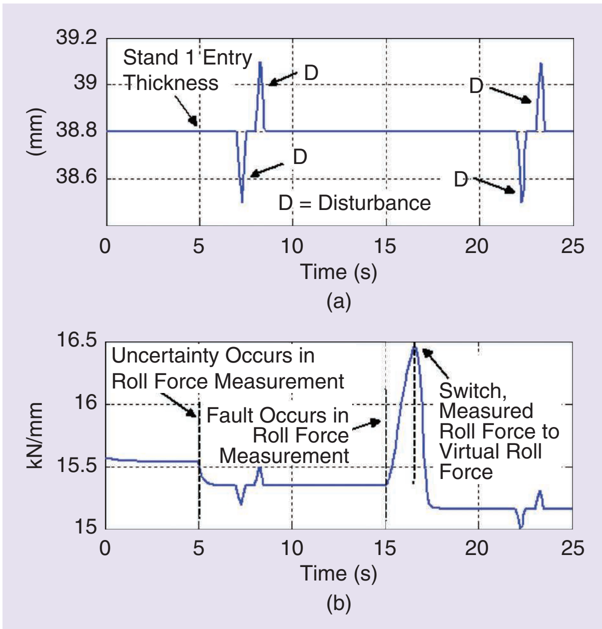

FIGURE 10. The specific roll force response to disturbances in entry thickness, with uncertainties [6]. (a) Disturbances in entry strip thickness, stand 1, and (b) actual specific roll force, stand 1.

to virtual tension. The resulting peak excursion in the actual tension was about 10% above the reference tension, and the final value was about 9% below the reference tension, which are within the reasonable operating range of the actual tension. The excursions in the roll force are minor and about the same as during a fault in the tension measurement [Figure 5(a)]. The results are similar for other combinations of uncertainties and disturbances in the tension. Figure 12 depicts the addition of unmodeled disturbances in the looper torque. These disturbances are well handled for measured and virtual tension, as shown in Figure 12.

In an additional simulation, a fault in the tension measurement occurring concurrently with the fault in the roll force measurement was addressed. Such a scenario was handled well by the controller. The results showed a slightly more significant effect on the tension and on the roll force. However, it is of lesser concern because in reality, it is extremely unlikely that a single credible initiating event can happen to cause both faults to occur simultaneously.

Conclusion

The initial work described here shows that the control technique performs well. The results of these simulations can be extended to evaluate other combinations of similar faults in the measurements of roll force, tension, and others that can be represented by a virtual rolling function. Future work will also consider recovery to normal operation following a faulted condition.

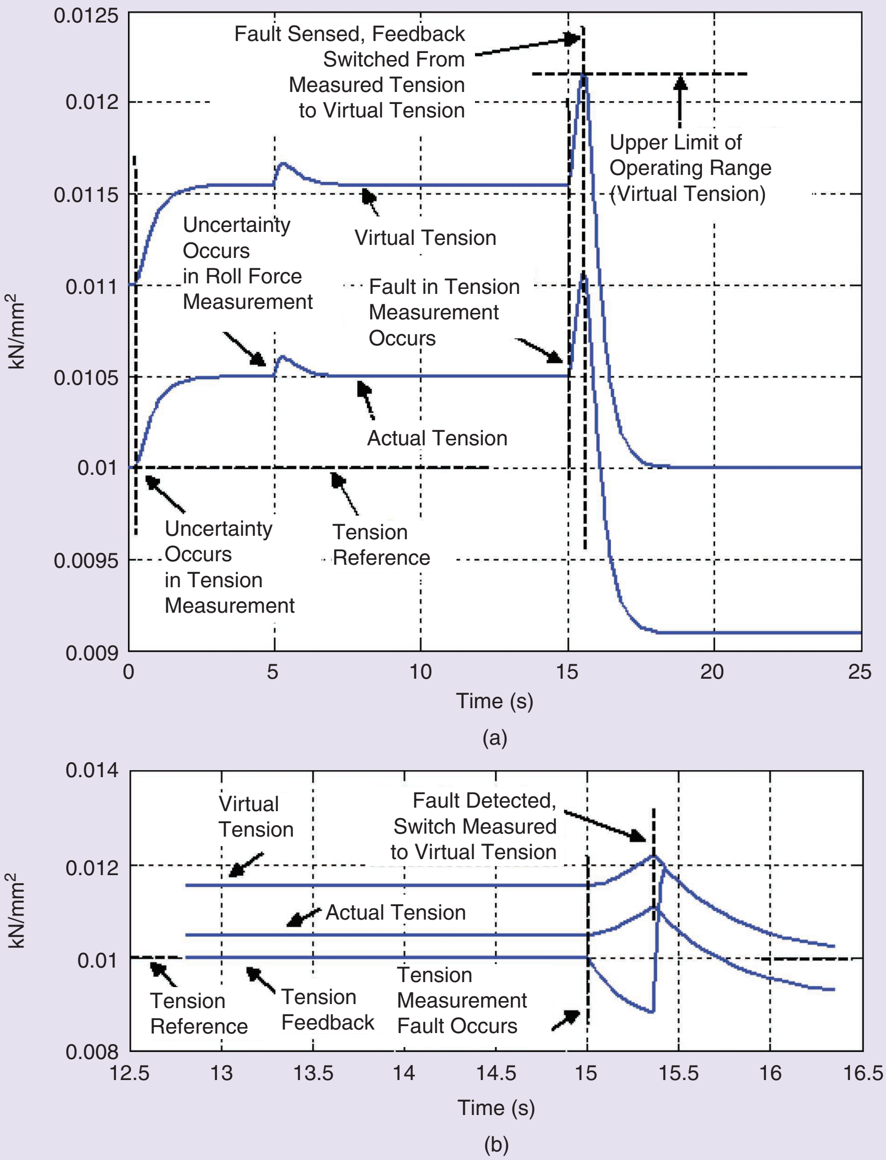

FIGURE 11. (a) The virtual and actual tension responses to a fault in tension measurement, with uncertainties, stands 1 and 2 [6]. (b) Detail of responses to a fault in tension measurement, with uncertainties, stands 1 and 2 during transfer from measured to virtual tension [6].

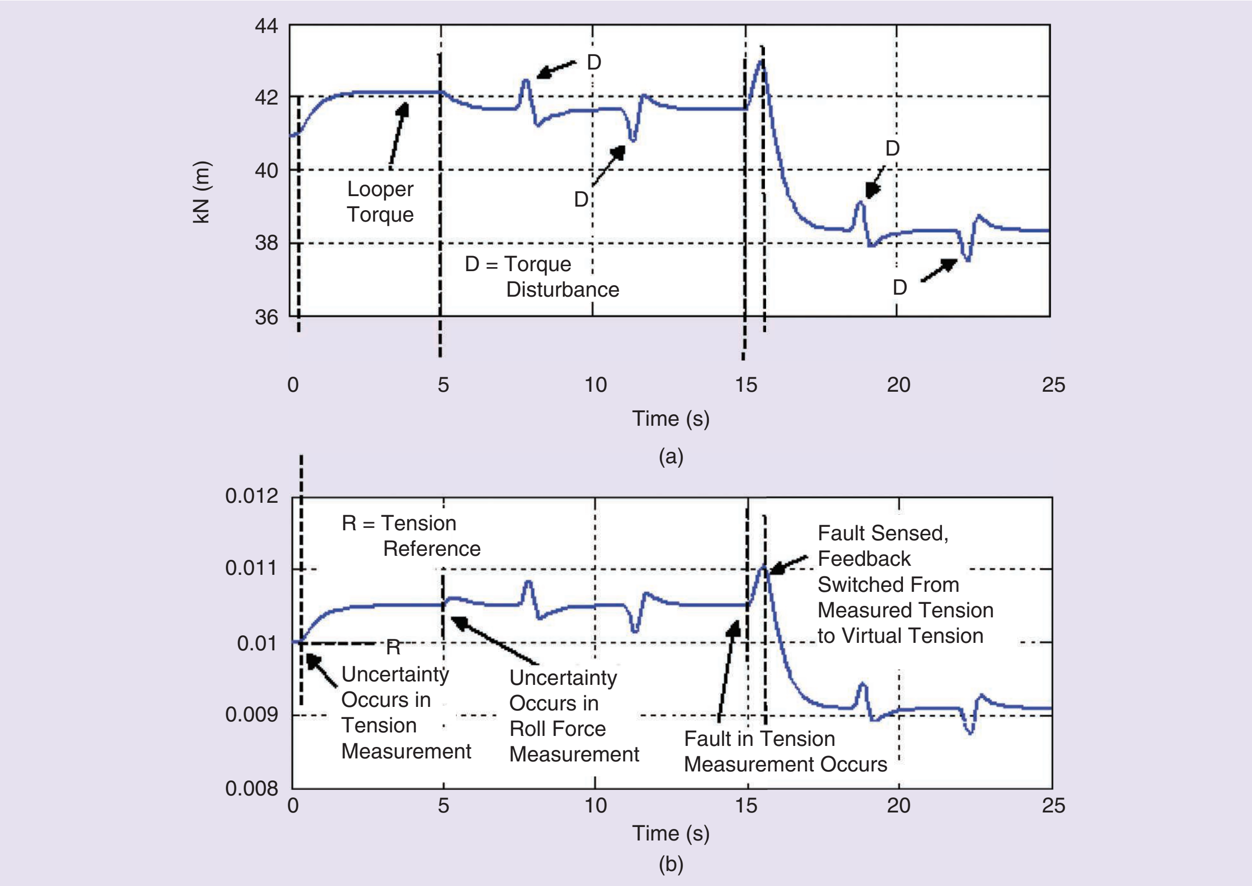

FIGURE 12. The tension response to unmodeled disturbances in looper torque, with uncertainties [6]: (a) disturbances in looper torque, stands 1 and 2, and (b) tension stress with disturbances in looper torque, stands 1 and 2.

Author Information

John Pittner (jrpst16@pitt.edu) is with the University of Pittsburgh, Pennsylvania. ***Marwan A. Simaan*** is with the University of Central Florida, Orlando. Pittner is a Senior Member of the IEEE. Simaan is a Life Fellow of the IEEE. This article first appeared as "Improving the Availability of Tandem Hot Metal Strip Rolling by the Use of Fault-Tolerant Techniques with Virtual Rolling" at the 2017 IEEE IAS Annual Meeting. This article was reviewed by the IAS Metals Industry Committee.

References

[1] J. Pittner and M. A. Simaan, *Tandem Cold Metal Rolling Mill Control*. New York: Springer-Verlag, 2011, ch. 5.

[2] J. Pittner and M. A. Simaan, "Improvement in control of the tandem hot strip mill," *IEEE Trans. Ind. Appl.*, vol. 49, no. 5, pp. 1962–1970, 2013.

[3] J. Pittner and M. A. Simaan, "Use of advanced control with virtual rolling to improve the control of the threading of the tandem hot metal strip mill," in *Proc. 2016 IEEE Industry Application Society Annu. Meeting*, Portland, OR, 2016, pp. 1–8.

[4] J. Pittner and M. A. Simaan, "A useful control model for tandem hot metal strip rolling," *IEEE Trans. Ind. Appl.*, vol. 46, no. 6, pp. 2251–2258, 2010.

[5] J. Pittner and M. A. Simaan, "An initial model for control of a tandem hot metal strip rolling process," *IEEE Trans. Ind. Appl.*, vol. 46, no. 1, pp. 46–53, 2010.

[6] J. Pittner and M. A. Simaan, "Use of fault-tolerant techniques with virtual rolling to improve the robustness to measurement faults in the control for tandem hot metal strip rolling," in *Proc. 2017 IEEE Industry Application Society Annu. Meeting*, Cincinnati, OH, 2017, pp. 1–8.

[7] M. Pietrzyk and J. G. Lenard, *Thermal-Mechanical Modeling of the Flat Rolling Process*. New York: Springer-Verlag, 1991, pp. 135–136.

[8] R. B. Sims, "The calculation of roll force and torque in hot rolling mills," *Proc. Inst. Mech. Eng.*, vol. 168, pp. 191–200, June 1954.

[9] M. Pietrzyk and J. G. Lenard, *Thermal-Mechanical Modeling of the Flat Rolling Process*. New York: Springer-Verlag, 1991, pp. 12–13.

[10] J. G. Lenard, M. Pietrzyk, and L. Cser, *Mathematical and Physical Simulation of Hot Rolled Products*. Amsterdam, The Netherlands: Elsevier, 1999, p. 91.

[11] H. Ford, E. F. Ellis, and D. R. Bland, "Cold rolling with strip tension, part I-A: New approximate method of calculation and comparison with other methods," *J. Iron Steel Inst.*, vol. 168, pp. 57–72, May 1951.

[12] W. L. Roberts, *Hot Rolling of Steel*. New York: Marcel Dekker, 1983, p. 782.

[13] M. A. Johnson, G. Hearns, and T. Lee, "The hot strip rolling mill looper: A control study," in *Mechatronic Systems Techniques and Applications, Industrial Manufacturing*, vol. 1, C. T. Leondes, Ed. New York: Gordon and Breach, 2000, pp. 169–253.

[14] T. Cimen, "Systematic and effective design of nonlinear feedback controllers via the state-dependent Riccati (SDRE) method," *Annu. Rev. Control*, vol. 34, no. 1, pp. 32–51, 2010.

[15] T. Cimen, "Survey of state-dependent Riccati equations in nonlinear feedback control synthesis," *J. Guidance Control Dynamics*, vol. 35, no. 4, pp. 1025–1047, 2012.

[16] T. Cimen, "On the existence of solutions characterized by Riccati equations to infinite-time horizon nonlinear optimal control problems," *IFAC Proc. Volumes*, vol. 44, no. 1, pp. 9618–9626, 2011.

[17] J. R. Cloutier and D. T. Stansbery, "The capabilities and art of state-dependent Riccati equation-based design," in *Proc. American Control Conf.*, Anchorage, Alaska, vol. 1, 2002, pp. 86–91.

[18] J. R. Cloutier, N. D'Souza, and C. P. Mracek, "Nonlinear regulation and nonlinear H∞ control via the state-dependent Riccati equation technique: Part 1, theory," in *Proc. Int. Conf. Nonlinear Problems in Aviation and Aerospace*, 1996, pp. 117–131.